

# RSC Advances



This is an *Accepted Manuscript*, which has been through the Royal Society of Chemistry peer review process and has been accepted for publication.

*Accepted Manuscripts* are published online shortly after acceptance, before technical editing, formatting and proof reading. Using this free service, authors can make their results available to the community, in citable form, before we publish the edited article. This *Accepted Manuscript* will be replaced by the edited, formatted and paginated article as soon as this is available.

You can find more information about *Accepted Manuscripts* in the [Information for Authors](#).

Please note that technical editing may introduce minor changes to the text and/or graphics, which may alter content. The journal's standard [Terms & Conditions](#) and the [Ethical guidelines](#) still apply. In no event shall the Royal Society of Chemistry be held responsible for any errors or omissions in this *Accepted Manuscript* or any consequences arising from the use of any information it contains.

## ARTICLE

# A new method for synthesis of $\text{LiNi}_{1/3}\text{Co}_{1/3}\text{Mn}_{1/3}\text{O}_2$ from waste lithium ion batteries

Cite this: DOI: 10.1039/x0xx00000x

Lu Yao<sup>a</sup>, Yong Feng<sup>a</sup>, Guoxi Xi<sup>a,b\*</sup>Received 00th January 2014,  
Accepted 00th January 2012

DOI: 10.1039/x0xx00000x

[www.rsc.org/](http://www.rsc.org/)

A new process for synthesis of  $\text{LiNi}_{1/3}\text{Co}_{1/3}\text{Mn}_{1/3}\text{O}_2$  from recycled valuable metals of waste lithium ion batteries (LIBs) is introduced herein. Citric acid was used as both a leaching and chelating agent. The overall process involves three steps: dissolution of spent lithium ion batteries, the sol-gel formation and  $\text{LiNi}_{1/3}\text{Co}_{1/3}\text{Mn}_{1/3}\text{O}_2$  powder formation. The concentration of metal ions, specifically lithium, nickel, manganese, and cobalt in the leachate were determined by inductively coupled plasma optical emission spectroscopy (ICP-OES). The morphologies of the cathode material from waste LIBs before and after leaching, as well as those of the leaching residue and the final products, were observed by scanning electron microscopy (SEM). The structure of the final product was characterized by X-ray diffraction (XRD) analysis. As regards electrochemical properties, the re-synthesized and fresh-synthesized samples delivered capacities of 147 and 150 mAhg<sup>-1</sup>, respectively, in the first cycle. The rate performances, high and low temperature discharge performances, and the electrochemical impedance spectra (EIS) are also discussed. This study suggests that the waste lithium ion batteries can be recycled to re-synthesize new cathode materials with good electrochemical performance.

## 1. Introduction

Lithium ion batteries (LIBs) are currently extensively used as electrochemical power sources in aerospace applications and electric vehicles because of their high power and energy density, high cell voltage, long storage life, low self-discharge rate, and wide operating temperature range.<sup>1-3</sup> In recent years, increased production of electronic equipment and vehicles has led to more LIBs being manufactured, and hence a dramatic increase in the volume of depleted LIBs.

Waste LIBs not only contain many flammable organic chemicals, but also many valuable metals, such as cobalt, nickel, aluminum, lithium, and manganese, and these metals are normally present at very high concentrations.<sup>4,5</sup> Hence, waste LIBs represent an important secondary resource. Recycling of waste batteries has aroused widespread interest in recent years. Research has mainly focused on the recycling of waste LIBs with  $\text{LiCoO}_2$  as the cathode material, and many processes have been proposed for the recycling of cobalt from this source. The main processes for recycling waste LIBs are pyrometallurgy<sup>6-8</sup>, hydrometallurgy,<sup>4, 9-11</sup> and biometallurgy<sup>12-14</sup>. Pyrometallurgical processes are often accompanied by high gas emissions and have high energy consumption. The biometallurgical process is a very promising technology in terms of its high efficiency, low cost, and the modest apparatus needed, but the treatment period

is too long and the bacteria required are difficult to incubate.<sup>5</sup> Hence, the hydrometallurgy process has attracted the interest of many researchers and has become a focus of research work in recent years. Most of the hydrometallurgical methods involve acid leaching and the separation of metal ions. Sulfuric acid<sup>10, 15</sup>, nitric acid,<sup>16,17</sup> and hydrochloric acid<sup>18</sup> have high leaching efficiencies for cobalt and lithium. However, these strong acid solutions are liable to release  $\text{SO}_3$ ,  $\text{NO}_x$ , and  $\text{Cl}_2$ , respectively, and produce leachates of low pH, posing a threat to the environment and making them unfavorable for subsequent procedures. A number of organic acids are under development as potential leaching agent<sup>4,9,15,16,19</sup>. However, except for the complicated separation of the metal ions, there has been little research on the subsequent treatment of the leachates.

Nowadays, the main industrial cathode materials are  $\text{LiCoO}_2$ ,<sup>16</sup>  $\text{LiMn}_2\text{O}_4$ ,<sup>20, 21</sup>  $\text{LiNi}_x\text{Co}_y\text{Mn}_{1-x-y}\text{O}_2$  (LNCM),<sup>22, 23</sup> and  $\text{LiFePO}_4$ .<sup>24, 25</sup> Members of the LNCM family, with high discharge capacity, moderate voltage platform, and hence high energy density, have been considered as the most promising cathode candidates in recent years.<sup>22, 26-29</sup> Among them,  $\text{LiNi}_{1/3}\text{Co}_{1/3}\text{Mn}_{1/3}\text{O}_2$  is a unique material because of its high specific capability.<sup>30</sup> Its market share has increased year by year. However, research on the recycling of LNCM has been limited. The main research on recycling waste lithium ion batteries with LNCM as the cathode material has been focused on the recycling and separation of

metal ions by inorganic acid leaching.<sup>31</sup> Citric acid is inexpensive and non-hazardous, and could offer H<sup>+</sup> and carboxyl groups for the leaching process and subsequent chelating process. In this study, we have recycled waste LIBs through an environmentally friendly process involving citric acid, which avoids complicated metal ion separation procedures. Moreover, a cathode material, LiNi<sub>1/3</sub>Co<sub>1/3</sub>Mn<sub>1/3</sub>O<sub>2</sub>, with high added value has been synthesized by a very simple method.

## 2. Materials and methods

### 2.1 Materials and reagents

The spent LIBs used in our study were kindly donated by Henan Huanyu Group (Xinxiang, China). All reagents used in this study were of analytical grade, and the solutions were prepared at the specified concentrations in distilled water.

### 2.2 Experimental procedure

#### 2.2.1 Pre-treatment of the waste LIBs

The spent LIBs were firstly discharged to prevent short-circuiting and self-ignition, then dismantled manually into different components with appropriate safety precautions<sup>6</sup>. The cases and anodes were dealt with by other methods, which are not described herein. This work was mainly concerned with recycling of the cathode material with the composition LNCM.

**Immersion in *N*-methyl pyrrolidinone (NMP) and thermal treatment:** The cathodes were immersed in NMP<sup>4, 32</sup> and heated to 80°C for 1 h, and then transferred to an ultrasonic bath for 20 min. The ultrasonic treatment was intended to improve the efficiency and yield of separating the active cathode materials from the aluminum foils. The NMP extract was then filtered through a microfiltration membrane and the collected material was washed and dried at 100 °C. The recovered spent cathode material was calcined at 600°C for 4 h in a muffle furnace to burn off impurities such as carbon and polyvinylidene fluoride (PVDF). The obtained powder was then ground for 30 min in a planetary ball mill for easier leaching.

#### 2.2.2 Leaching of metal ions

The hydrometallurgical leaching experiments were carried out in a three-necked reactor, which was placed in a water bath to control the temperature. The reactor was fitted with a magnetic stirring apparatus. To determine the optimum conditions, different experimental conditions, including solid/liquid ratio (40–120 g/L), citric acid concentration (0.5–2.0 mol/L), H<sub>2</sub>O<sub>2</sub> concentration (0–25 vol.%), temperature (40–80 °C), and duration (10–80 min) were studied. The pH of the mixture during the leaching process was monitored with a pH meter. The insoluble residue was separated from the leachate by filtration.

#### 2.2.3 Synthesis of LiNi<sub>1/3</sub>Co<sub>1/3</sub>Mn<sub>1/3</sub>O<sub>2</sub>

The concentrations of lithium, nickel, cobalt, and manganese ions in the leachate were determined by ICP-OES. The molar ratio of these metal ions was adjusted to 3.05:1:1:1 at a total metal ion concentration of 1.0 mol L<sup>-1</sup> by adding LiNO<sub>3</sub>, Mn(NO<sub>3</sub>)<sub>2</sub> (50% solution), Ni(NO<sub>3</sub>)<sub>2</sub>·6H<sub>2</sub>O, and Co(NO<sub>3</sub>)<sub>2</sub>·6H<sub>2</sub>O and the pH was adjusted to 8.0 by adding a suitable amount of aqueous ammonia. The transparent solution was heated at 80 °C in a water bath to obtain a transparent gel, which was then dried at 110 °C in an oven for 24 h. The dried gel was calcined at 350 °C for 2 h in the ambient atmosphere and then at 750 °C for 12 h in a muffle furnace, and the final product was designated as re-synthesized LiNi<sub>1/3</sub>Co<sub>1/3</sub>Mn<sub>1/3</sub>O<sub>2</sub>. For comparison, stoichiometric amounts of LiNO<sub>3</sub>, Ni(NO<sub>3</sub>)<sub>2</sub>·6H<sub>2</sub>O, Co(NO<sub>3</sub>)<sub>2</sub>·6H<sub>2</sub>O and Mn(NO<sub>3</sub>)<sub>2</sub> (50% solution) were used as starting materials to synthesize LiNi<sub>1/3</sub>Co<sub>1/3</sub>Mn<sub>1/3</sub>O<sub>2</sub> by the same method. This product was designated as fresh-synthesized LiNi<sub>1/3</sub>Co<sub>1/3</sub>Mn<sub>1/3</sub>O<sub>2</sub>.

### 2.3 Analytical methods

The total metal ion concentration after acid leaching was determined by ICP-OES (model Optima 2100DV, USA). The microstructures of the cathode material before and after leaching were observed by SEM (Hitachi). Energy-dispersive X-ray spectroscopy (EDS) was carried out using an Oxford 7426 accessory as an SEM attachment, operated at an acceleration voltage of 20KV. The phase of samples was determined by XRD analysis (D8 Advance, Bruker AXS, Germany) using Cu-K<sub>α</sub> radiation. The electrochemical performances of the samples were studied by using CR2016-type coin cells. For the cathode assembly, LiNi<sub>1/3</sub>Co<sub>1/3</sub>Mn<sub>1/3</sub>O<sub>2</sub> powder was thoroughly mixed with PVDF as a binder and two conducting media (Super-P and KS-6) at a weight ratio of 80:10:5:5 in NMP to form an electrode slurry. This was pasted on an Al foil, the solvent was evaporated, and the prepared cathode sheets were dried in vacuo and pressed under a pressure of approximately 200 g m<sup>-2</sup>. Coin cells were then assembled in a glove box for electrochemical characterization. In the test cells, Li foil and a porous polypropylene film served as the counter electrode and the separator, respectively. The electrolyte was 1.0 mol L<sup>-1</sup> LiPF<sub>6</sub> in a mixture of ethylene carbonate, diethyl carbonate, and dimethyl carbonate with a weight ratio of 1:1:1. Charge/discharge experiments were performed on Land battery tests (Land CT2001A, Wuhan, China) between 2.75–4.25V. The assembled cells were tested for 50 cycles at the current density of 1 C (140 mA g<sup>-1</sup>) to analyze cycling performance. Various rates (0.2, 1, 2, 3 and 5 C) were also tested to investigate the rate capability of the samples. Discharge tests were performed at -20 °C, 25 °C and 55 °C to analyze the performance of materials at high and low temperature. Electrochemical impedance spectra (EIS) were recorded using an electrochemical workstation (CHI 660D, Shanghai, Chenghua Company, China).

## 3. Results and discussion

### 3.1 Pre-treatment of cathodes from spent LIBs

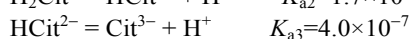
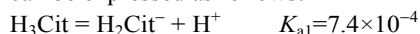
SEM images of the active materials obtained from the cathodes before and after calcination are shown in Fig.1a and b. Numerous small solid particles were seen between the active materials. These may have been of binder and conductor carbon added during manufacturing of the LIBs. It can be seen that most of these small particles vanished after calcination at 600 °C for 4h, which we attribute to their combustion. An image of the residue obtained after leaching with aqua regia is shown in Fig.1c, which reveals an amorphous structure. This may have been ash from combustion of the binder and conductor. Fig.1a', b' and c' show the corresponding EDS results. After calcination at 600 °C for 4 h, the weight ratio of carbon decreased significantly, which confirmed combustion of the binder and conductor. For the leaching residue, only three elements were detected, carbon at 70.87 wt%, oxygen at 19.37 wt% and a small amount of fluorine. No metal ions were detected in the residue. The elemental composition measured by EDS is listed in Table 1.

Table 1. Elemental compositions of the waste LNCM before and after calcination and of the leaching residue

Element	a: before calcined		b: after calcined		c: residue	
	wt%	At%	wt%	At%	wt%	At%
C	29.24	47.75	3.81	9.21	70.87	77.39
O	30.20	37.03	25.81	46.79	19.37	15.86
F	1.91	1.98	8.36	12.77	9.78	6.75
Ni	17.90	5.98	29.37	14.51		
Co	5.79	1.96	14.08	6.93		
Mn	14.96	5.34	18.56	9.80		

### 3.2 Leaching of waste LNCM

Citric acid is a common organic acid. Three carboxyl groups are contained in one  $C_6H_8O_7$  molecule. Theoretically, one mole of  $C_6H_8O_7$  could dissociate 3 moles of  $H^+$ . However, not all of the  $H^+$  is released to the solution; the ionizable hydrogen dissociates in a stepwise manner. The dissociation of citric acid can be expressed as follows:



$LiNi_{1/3}Co_{1/3}Mn_{1/3}O_2$  has the  $\alpha$ - $NaFeO_2$  structure with space group  $R3m$ , which is also characteristic of layered  $LiCoO_2$ . The valencies of nickel, cobalt, and manganese ions are +2, +3, and +4, respectively<sup>33</sup>. In the crystal lattice, lithium ions occupy the 3a sites, the other metal ions, namely nickel, cobalt, and manganese, randomly occupy the 3b sites, and oxide anions occupy the 3c sites. Each transition metal ion is surrounded by six oxygen atoms, forming an  $MO_6$  octahedral structure, which

is very stable. The reaction between LNCM and citric acid is a multiphase process. The chemical bonds between M (nickel,

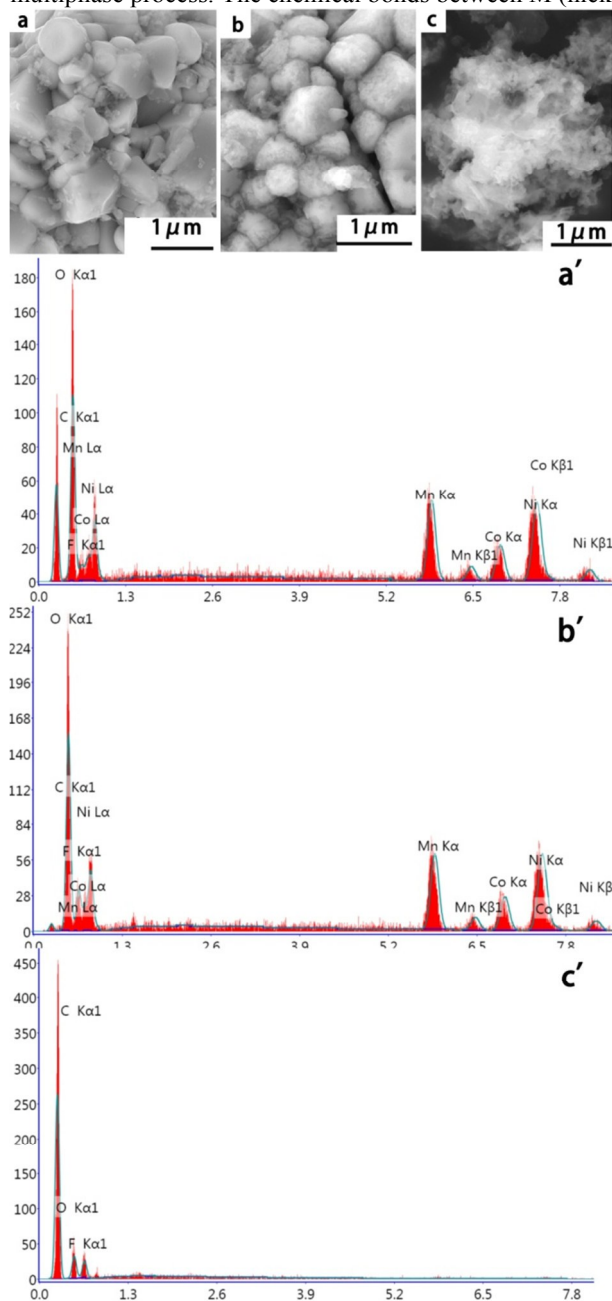


Fig.1 SEM and EDS images of the waste LNCM: (a) the waste cathode material before calcination, (b) the cathode material after calcination and (c) the leaching residue.

manganese, cobalt) and oxygen are extremely strong, which makes it difficult to leach with an organic acid. During the leaching process, one hydrogen ion can displace one lithium ion from LNCM. For  $L_{1-x}NMC$ , during the charge/discharge process, different values of  $x$  give rise to different redox reactions. When  $x$  is between 0 and 1/3, the redox reaction of  $Ni^{2+}/Ni^{3+}$  occurs. When  $x$  is between 1/3 and 2/3, the redox reaction of  $Ni^{3+}/Ni^{4+}$  occurs. The main metal ions contained in the waste electrode are thus likely to be  $Li^+$ ,  $Ni^{2+}$ ,  $Ni^{3+}$ ,  $Ni^{4+}$ ,  $Co^{2+}$ ,  $Co^{3+}$ , and  $Mn^{4+}$ . Of these,  $Li^+$ ,  $Ni^{2+}$ , and  $Co^{2+}$

may be readily leached by the acid, but  $\text{Ni}^{3+}$ ,  $\text{Ni}^{4+}$ ,  $\text{Co}^{3+}$ , and  $\text{Mn}^{4+}$  would not be readily leached without a reducing agent. There are some reports that hydrogen peroxide ( $\text{H}_2\text{O}_2$ ), can be oxidized by high-valent transition metal ions. For the recycling of  $\text{LiCoO}_2$ , on adding  $\text{H}_2\text{O}_2$  to citric acid, the leaching efficiencies of cobalt and lithium increased from 37% and 54% to 93% and 99%, respectively<sup>19</sup>. In similar studies, on adding  $\text{H}_2\text{O}_2$  in malic acid, aspartic acid and sulfuric acid, the leaching efficiencies of cobalt and lithium also increased dramatically<sup>4,34,35</sup>. It is beneficial to deploy a reducing agent along with leaching acids. H. Zhou *et al* found that waste  $\text{LiNi}_{1/3}\text{Co}_{1/3}\text{Mn}_{1/3}\text{O}_2$  could be dissolve in  $4\text{molL}^{-1}$  sulfuric acid with 30 wt%  $\text{H}_2\text{O}_2$ , and the leaching equation was as follows<sup>36</sup>:

$$6\text{LiNi}_{0.33}\text{Mn}_{0.33}\text{Co}_{0.33}\text{O}_2 + 9\text{H}_2\text{SO}_4 + \text{H}_2\text{O}_2 = 2\text{MnSO}_4 + 2\text{NiSO}_4 + 2\text{CoSO}_4 + 3\text{Li}_2\text{SO}_4 + 2\text{O}_2 + 10\text{H}_2\text{O}$$

$\text{H}_2\text{O}_2$  serves as a reductant in this system,  $\text{Ni(IV)}$  serves as an oxidant,  $\phi^{\ominus}\text{Ni(IV)/Ni}^{2+} = 1.678\text{V}$ ,  $\phi^{\ominus}\text{O}_2/\text{H}_2\text{O}_2 = 0.699\text{V}$ ,  $\Delta E^{\ominus} = \phi^{\ominus}\text{Ni(IV)/Ni}^{2+} - \phi^{\ominus}\text{O}_2/\text{H}_2\text{O}_2 = 0.979\text{V}$ ,  $\lg K = n\Delta E^{\ominus}/0.059 = 33$ ,  $K = 10^{33}$ . The stability constant  $K$  is sufficiently high and this redox reaction could proceed effectively. Similarly,  $\text{Mn(IV)}$  and  $\text{Co(III)}$  could also be reduced by  $\text{H}_2\text{O}_2$  in the citric acid solution.

So, in our experiment, we chose  $\text{H}_2\text{O}_2$  to accelerate the leaching rates and efficiency. Thus the dissolution of nickel, manganese and cobalt ions follows a reduction-complex mechanism:  $\text{M}^{3+/4+}\{\text{oxide}\} + \text{H}^+ + \text{H}_2\text{O}_2 \rightarrow \text{M}^{2+}\{\text{oxide}\} \rightarrow \text{M}^{2+}\{\text{aq}\} \rightarrow \text{M(II)-citrate}$ , (where  $\text{M}$  represents either nickel, cobalt or manganese)<sup>37</sup>. Such a heterogeneous reaction is expected to occur at the interface of solid (oxide lattice) and liquid. As the metal ions dissolves, the crystal lattice is disturbed. At the same time, the surrounding  $\text{M}$  ions may be leached into solution through complexation. All of the transition metal ions in this system, namely cobalt, nickel and manganese can be expected to form citrate complexes, because citrate is a strong complexing agent and was deployed in a stoichiometric amount (assuming 1:2 metal-to-ligand ratio)<sup>38</sup>. The leaching mechanism is shown schematically in Fig.2.

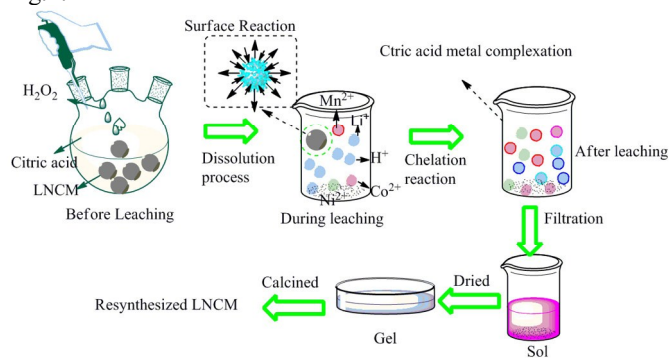


Fig.2 Schematic representation of the leaching mechanism and the process.

### 3.2.1. Effect of acid concentration on leaching efficiency

We studied the effect of acid concentration on the leaching efficiency of waste LNCM. The concentration of citric acid was

varied from  $0.5$  to  $2.0\text{molL}^{-1}$  at a reaction temperature of  $60^\circ\text{C}$ , a duration of  $40\text{min}$ , and an  $\text{H}_2\text{O}_2$  concentration of  $12\text{vol.}\%$ . From Fig.3a, it can be seen that the leaching efficiency of the waste LNCM increased dramatically with increasing citric acid concentration up to  $1.0\text{molL}^{-1}$ , whereupon more than 98% of the metal ions were leached. When the citric acid concentration was further increased from  $1.0\text{molL}^{-1}$  to  $2.0\text{molL}^{-1}$ , the leaching efficiency increased only very slightly. Hence, we chose  $1.0\text{molL}^{-1}$  as the optimum citric acid concentration for the leaching process.

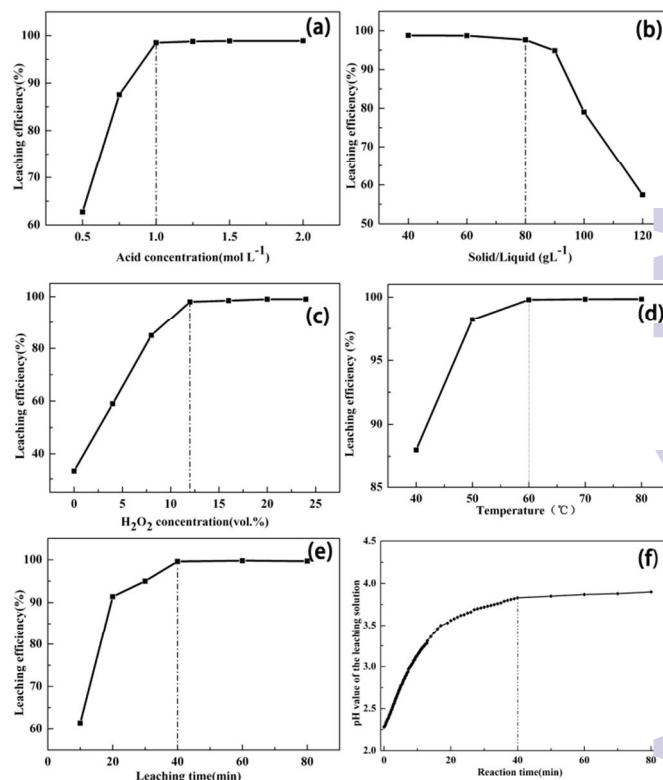


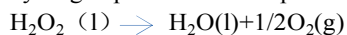
Fig.3 Impact of leaching conditions on leaching efficiency of waste LNCM: (a) citric acid concentration, (b) solid/liquid ratio (c)  $\text{H}_2\text{O}_2$  concentration, (d) temperature and (e) reaction time; (f) curve of pH value of the solution vs. reaction time.

### 3.2.2. Dissolution of the waste cathode material at different solid/liquid ratios

To determine the effect of solid-to-liquid ratio (S:L) on the leaching efficiency, experiments were conducted at S:L from  $40\text{gL}^{-1}$  to  $120\text{gL}^{-1}$ , keeping the other parameters fixed as follows: leaching temperature  $60^\circ\text{C}$ , citric acid concentration  $1.0\text{molL}^{-1}$ ,  $\text{H}_2\text{O}_2$  concentration  $12\text{vol.}\%$ , and a duration of  $40\text{min}$ . Fig.3b shows that the leaching efficiency decreased dramatically with increasing S:L. As S:L below  $60\text{gL}^{-1}$ , more than 98% of the waste LIB cathode material was leached. When the S:L exceeded  $80\text{gL}^{-1}$ , however, the leaching efficiency decreased sharply. To achieve the best compromise between leaching efficiency and lower chemical consumption, leaching with a solid/liquid ratio of  $80\text{gL}^{-1}$  was determined to be optimal.

### 3.2.3 Effect of hydrogen peroxide concentration

Experiments were conducted in the hydrogen peroxide concentration range from 0 to 25 vol.%, maintaining the citric acid concentration at  $1.0 \text{ mol L}^{-1}$ , a solid/liquid ratio of  $80 \text{ g L}^{-1}$ , a temperature of  $60 \text{ }^\circ\text{C}$ , and a reaction time of 40 min. Fig.3c shows that the concentration of  $\text{H}_2\text{O}_2$  dramatically influenced the leaching efficiency. In the absence of  $\text{H}_2\text{O}_2$ , the leaching efficiency of the waste LNCM from waste LIBs was only 33.6%. When the concentration of  $\text{H}_2\text{O}_2$  was increased to 12%, the leaching efficiency increased to 98.1%. On further increasing the  $\text{H}_2\text{O}_2$  concentration to 24 vol.%, there was no significant change in the leaching efficiency. According to Ferreira's theory,<sup>35</sup> the effect of  $\text{H}_2\text{O}_2$  was possibly related to some change in the leaching kinetics of  $\text{LiCoO}_2$ . In this system, the dissolution of LNCM involves the reduction of  $\text{Co}^{3+}$ ,  $\text{Ni}^{3+}$ ,  $\text{Ni}^{4+}$ , and  $\text{Mn}^{4+}$  in the solid to  $\text{Co}^{2+}$ ,  $\text{Ni}^{2+}$ , and  $\text{Mn}^{2+}$  in the aqueous phase. The leaching efficiency of 33.6% in the absence of  $\text{H}_2\text{O}_2$  may be attributed to  $\text{Li}^+$  ions and a small amount of divalent metal ions ( $\text{Co}^{2+}$ ,  $\text{Ni}^{2+}$ ) being leached. Thus, in this system, the requisite amount of  $\text{H}_2\text{O}_2$  needed to reduce the high-valent metal ions to divalent ions was about 12 vol.%. Excess hydrogen peroxide decomposed as follows upon heating:



Hence, when more  $\text{H}_2\text{O}_2$  was added, it had no significant influence on the leaching efficiency of the waste LIBs.

### 3.2.4 Effects of temperature and reaction time

The effects of the reaction temperature and time on the leaching efficiencies were studied, keeping the citric acid and  $\text{H}_2\text{O}_2$  concentrations fixed at  $1.0 \text{ mol L}^{-1}$  and 12 vol.%, respectively, and the solid/liquid ratio at  $80 \text{ g L}^{-1}$ . Leaching was then conducted in the temperature range  $40\text{--}80 \text{ }^\circ\text{C}$  for 10–60 min. The results are shown in Figs. 3d and 3e. They indicate that increasing the reaction temperature and time greatly enhanced the leaching efficiencies. The leaching efficiency of waste LNCM increased from 87.4% to 98.7% when the temperature was increased from  $40$  to  $60 \text{ }^\circ\text{C}$ . The leaching efficiency also increased from 61.3% to 98.7% when the duration was increased from 10 min to 40 min. Further increases in the leaching temperature and duration made no further contribution to the leaching efficiencies. We also tested the pH value during the leaching process and found it to increase from 2.28 to 3.90. The trend in the leaching efficiency versus reaction time is similar to that in pH versus reaction time, as shown in Fig.3e and 3f. From the viewpoint of low energy consumption and high yield, we chose  $60 \text{ }^\circ\text{C}$  as the optimum reaction temperature, with a duration of 40 min.

### 3.3 Synthesis and characterization of $\text{LiNi}_{1/3}\text{Co}_{1/3}\text{Mn}_{1/3}\text{O}_2$

An aliquot (15 mL) of the solution obtained after acid leaching and filtration was placed in a conical flask. The metal ion ratio was adjusted to 3.05:1:1 at a total metal ion concentration of  $1.0 \text{ mol L}^{-1}$  by adding  $\text{LiNO}_3$ ,  $\text{Ni}(\text{NO}_3)_2 \cdot 6\text{H}_2\text{O}$ ,  $\text{Co}(\text{NO}_3)_2 \cdot 6\text{H}_2\text{O}$  and  $\text{Mn}(\text{NO}_3)_2$  (50% solution) as required. The solution was

adjusted to pH 8.0 and stirred for 5 min. Another aliquot (15 mL) of the solution was used as a control. The two solutions were concentrated to dryness by freeze-drying. SEM images of the respective powders are shown in Figs.4a and 4b. In Fig.4b, it can be seen that the powder had a highly reticulated structure. This may be ascribed to the increased pH, which facilitated the second and third ionizations of citric acid, so that the system could supply more carboxyl groups to coordinate to the metal ions. The SEM image shows that a large reticular complex was formed when the solution was adjusted to pH 8.0 with aqueous ammonia, in accordance with the dissociation mechanism of citric acid.

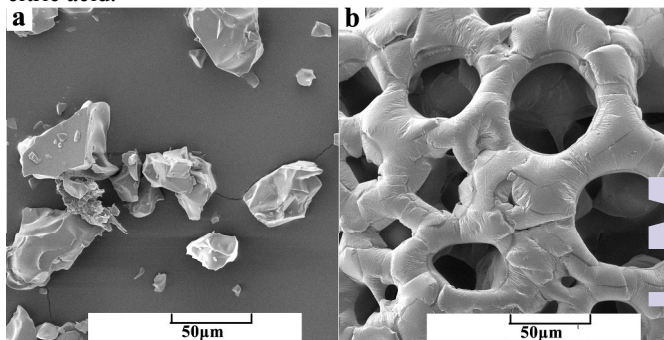


Fig.4 SEM images at different stage of the process: (a) the freeze-dried compound obtained from the leachate, (b) the freeze-dried compound obtained after adjusting the pH of the leachate to 8.0.

### 3.3.1 XRD and SEM characterizations

The XRD patterns (Fig.5) of the re-synthesized and fresh-synthesized LNCM materials showed that both the samples had the layered structure without any impurity reflections. All the peaks could be indexed to the hexagonal  $\alpha\text{-NaFeO}_2$  crystal structure with a space group of  $R\bar{3}m$ . The sharp and well-defined diffraction peaks indicated good crystallization. The clear splitting of the hexagonal doublets (006/102) around  $38^\circ$  and the (108)/(110) around  $65^\circ$  observed for the samples indicate the highly ordered layered structure of  $\text{LiNi}_{1/3}\text{Co}_{1/3}\text{Mn}_{1/3}\text{O}_2$ .<sup>22, 39</sup>

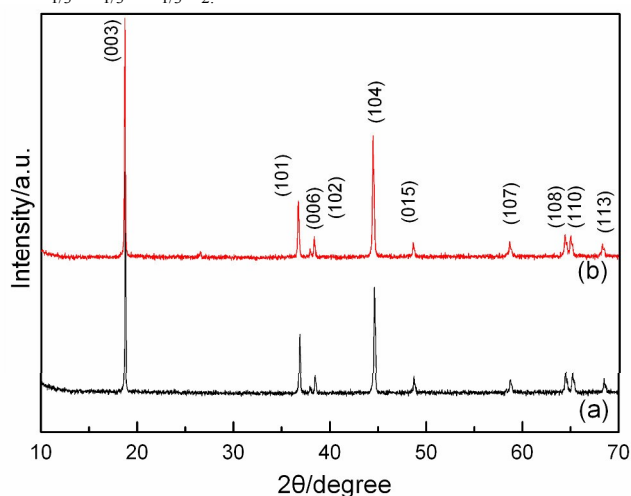


Fig.5. XRD patterns of the synthesized samples: (a) the re-synthesized sample, (b) the fresh-synthesized sample.

SEM images of the re-synthesized and fresh-synthesized samples are shown in Fig.6. No obvious differences between the two samples were apparent from SEM observation. Both the two powders consisted of well-crystallized relatively globular particles with smooth surfaces and uniform distributions. The particle diameters of the two samples were about 100-200nm. In general, a small particle size can accelerate lithium-ion reactions between the electrode material and the electrolyte by reducing the diffusion path of lithium ions inside the particle, and the lithium ions can be easily inserted into and extracted from their sites or into defects. A small particle size of the cathode material is an important factor, as it gives a high surface area and greatly influences the electrochemical properties, such as rate capability and discharge capacity.

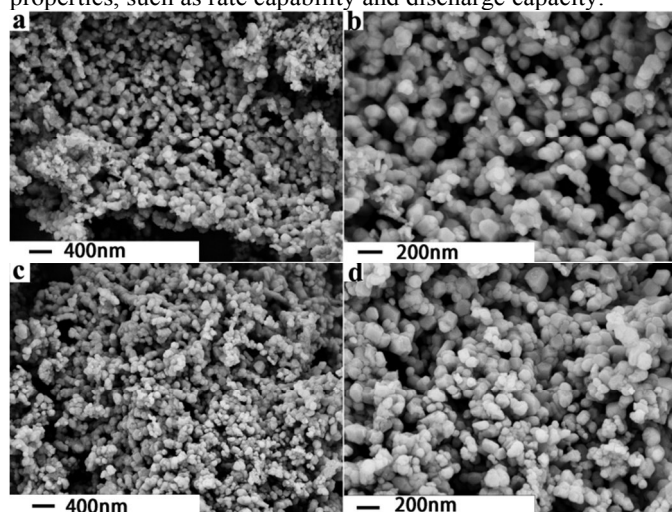


Fig.6 SEM images of re-synthesized and fresh-synthesized samples prepared by sol-gel method at magnifications of  $\times 50K$  and  $100K$ : (a, b) re-synthesized sample; (c, d) fresh-synthesized sample.

### 3.2 Electrochemical performance

In order to systematically evaluate the electrochemical performance of the samples, a series of electrochemical tests were performed. Charge/discharge profiles of the 1st, 2nd, 3rd, 10th, 20th, 50th cycles are shown in Fig.7a. The re-synthesized and fresh-synthesized samples delivered capacities of 147 and  $150\text{mAhg}^{-1}$ , respectively, in the first cycle. Fig.7b shows the cycle properties of the re-synthesized and fresh-synthesized  $\text{LiNi}_{1/3}\text{Co}_{1/3}\text{Mn}_{1/3}\text{O}_2$  samples between 2.75 and 4.25V. No difference in the cycle performances of the two samples can be discerned. Both of the samples showed good cycling properties, and the capacity retention after 50 cycles reached 93%.

The rate performances of the re-synthesized sample were incrementally tested from 0.2C to 5 C (Fig.7c). The discharge capacities of the re-synthesized sample were measured as 154.2, 147.0, 140.0, 136.7 and  $108.6\text{mAhg}^{-1}$  at 0.2, 1, 2, 3 and 5 C,

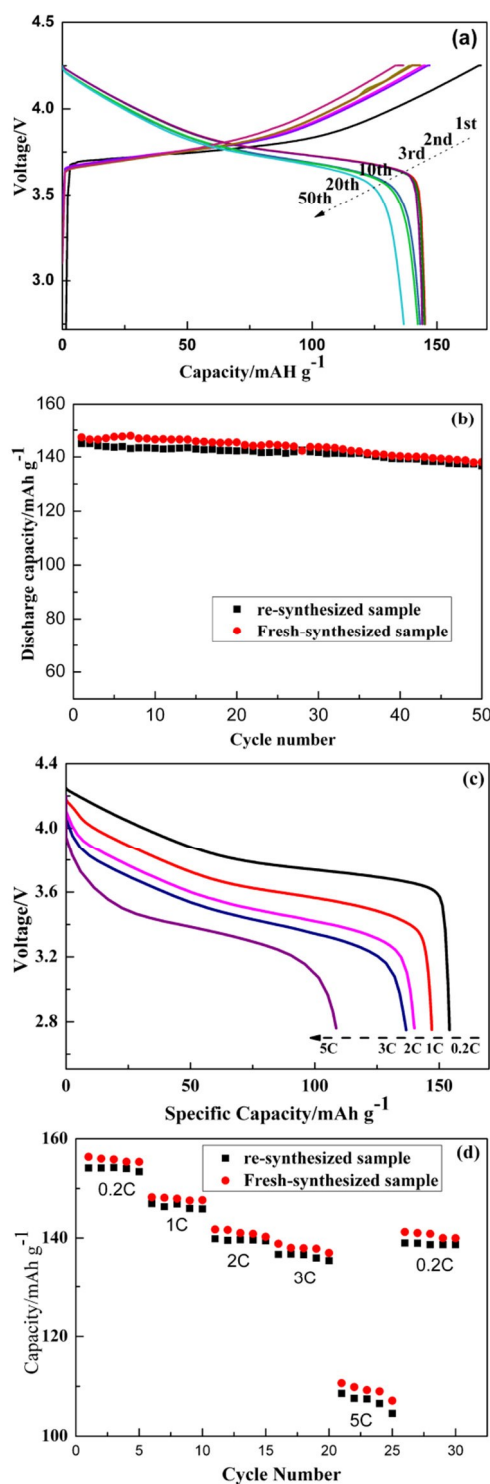


Fig.7 Cycling and rate performances of LNCM: (a) charge-discharge curves of re-synthesized sample at 1 C, (b) cycling performance comparison of the re-synthesized and fresh-synthesized sample at 1 C, (c) discharge curves of re-synthesized sample at different rates, (d) rate capabilities of the re-synthesized and fresh-synthesized samples, respectively. At low charge-discharge rates, the discharge curves were flat and smooth, indicating that the electrolyte suitably surrounded the particles and electrolyte transfer could maintain the electrochemical process. At a relatively high

charge–discharge rate (2 or 3 C), the electrolyte insufficiently surrounded the particles to support the electrochemical process, leading to a concentration polarization during electrolyte transfer. Thus, it produced a polarization effect on discharge curves. The small diameters and good dispersal of the particles facilitated electrolyte transfer, so a slow drop in discharge curves was observed. When the discharge rate reached 5 C, the electrochemical process was too fast. The electrolyte in pores was insufficient to support the electrochemical process, and therefore a serious polarization was generated, and the discharge curve showed an obvious drop.<sup>40</sup> The rate capabilities of the re-synthesized and fresh-synthesized samples are compared in Fig.7d. The average discharge capacities of the re-synthesized sample were 153.9, 146.4, 139.6, 113.5 and 106.9 mA h g<sup>-1</sup> at 0.2, 1, 2, 3, and 5 C, respectively. When the discharge rate was returned to 0.2 C, about 90.1% (138.8 mA h g<sup>-1</sup>) of the discharge capacity was recovered. The freshly synthesized sample showed the same trends and there were no obvious differences between the two samples.

The discharge performances at high and low temperatures are shown in Fig. 8a. Discharge of the re-synthesized sample at -20, 25, and 55 °C led to discharge capacities of 105.8, 140.5, and 144.6 mA h g<sup>-1</sup>, respectively. It can clearly be seen that the discharge capacity increased with increasing temperature, especially below 25 °C. Concomitantly, the discharge voltage increased dramatically on increasing the temperature from -20 to 25 °C. On further increasing the temperature from 25 to 55 °C, there were no obvious increase in capacity or voltage.

EIS tests were conducted and the impedance plots are shown in fig.8b. Both samples exhibited typical Nyquist characteristic. The intercept in the high frequency region of the Z real axis corresponds to the ohmic resistance (R<sub>s</sub>), the combined resistance of the electrolyte and the contacts of the cell. The semicircle at middle frequency is correlated with the Li<sup>+</sup> charge transfer resistance at the interface<sup>41</sup>. The inclined line in the lower frequency region represents the Warburg impedance (Z<sub>w</sub>), which is associated with the diffusion of Li<sup>+</sup> in LiNi<sub>1/3</sub>Co<sub>1/3</sub>Mn<sub>1/3</sub>O<sub>2</sub> particles<sup>42</sup>.

#### 4 Conclusions

A simple and environmentally friendly recycling process has been developed for the recovery of lithium, cobalt, nickel, and manganese from waste LIBs. The process avoids complicated separation of the metal ions and produces minimal pollution and side products. The optimum leaching conditions were determined to be as follows: citric acid concentration 1.0 mol L<sup>-1</sup>, solid-to-liquid ratio 80 g L<sup>-1</sup>, hydrogen peroxide concentration 12 vol.%, leaching temperature 60 °C, and reaction time 40 min. Under these conditions, more than 98% of the waste LIB cathode material could be leached. The leaching mechanism has been investigated from the viewpoint of the structure and dissociation mechanism of citric acid. The recovered and reconstituted cathode material showed high specific capacity, good rate and the cycling performances,

almost matching those of the fresh-synthesized LiNi<sub>1/3</sub>Co<sub>1/3</sub>Mn<sub>1/3</sub>O<sub>2</sub>.

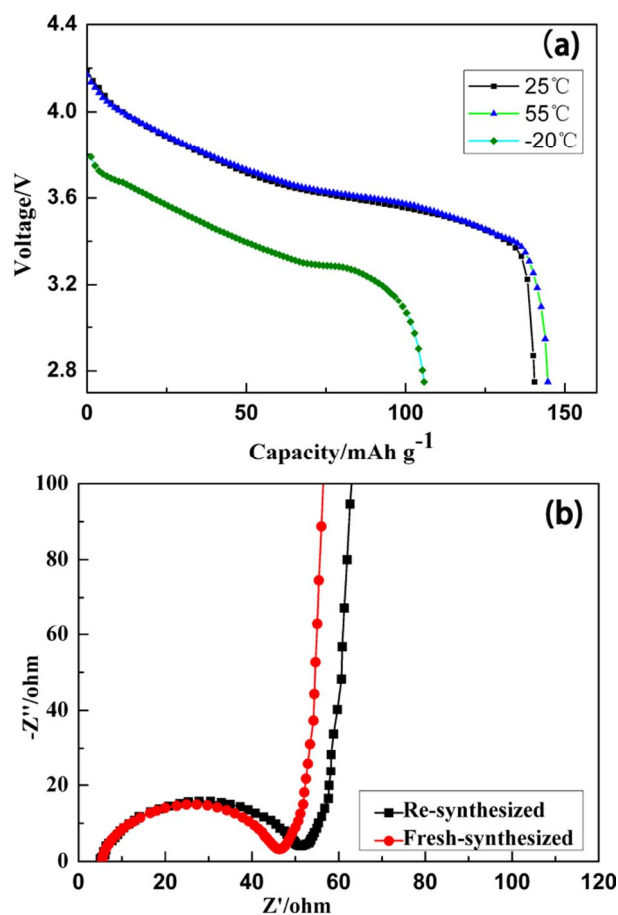


Fig.8 (a) Discharge profiles of the re-synthesized sample at -20, 25 and 55 °C at 1 C, (b) EIS plots of the re-synthesized and fresh-synthesized samples in fresh coin cells.

#### Acknowledgements

This study was supported by the National Science Foundation of China (No. 51174083). It was also supported by the Specialized Research Fund for the Doctoral Program of Higher Education (No. 20114104110004).

#### Notes and references

<sup>a</sup> School of Environment, Henan Normal University, Xinxiang 453007, PR China

<sup>b</sup> School of Chemistry and Chemical Engineering, Henan Normal University, Xinxiang 453007, PR China

Footnotes <sup>1</sup> Corresponding author. Tel.: +86 373 3325796/+8613937399599; fax: +86 373 3326336

E-mail addresses: [yaolu1020@126.com](mailto:yaolu1020@126.com) (L. Yao), [yaolu001@163.com](mailto:yaolu001@163.com) (G. Xi).



1. V. Etacheri, R. Marom, R. Elazari, G. Salitra and D. Aurbach, *Energy & Environmental Science*, 2011, **4**, 3243.
2. H. J. Bruno Scrosati B, Sun YK, *Energy & Environmental Science*, 2011, **4**, 3287.
3. D. Liu, W. Zhu, J. Trotter, C. Gagnon, F. Barray, A. Guerfi, A. Mauger, H. Groult, C. M. Julien, J. B. Goodenough and K. Zaghib, *RSC Adv.*, 2014, **4**, 154.
4. L. Li, J. Ge, R. Chen, F. Wu, S. Chen and X. Zhang, *Waste management*, 2010, **30**, 2615.
5. X. Zhang, Y. Xie, X. Lin, H. Li and H. Cao, *Journal of Material Cycles and Waste Management*, 2013, **15**, 420.
6. J. F. Paulino, N. G. Busnardo and J. C. Afonso, *Journal of hazardous materials*, 2008, **150**, 843.
7. L. Sun and K. Qiu, *Journal of hazardous materials*, 2011, **194**, 378.
8. H. Nie, L. Xu, D. Song, J. Song, X. Shi, X. Wang, and Z. Yuan, *Green Chemistry*, 2015, **17**, 1276.
9. L. Sun and K. Qiu, *Waste management*, 2012, **32**, 1575.
10. M. K. Jha, A. Kumari, A. K. Jha, V. Kumar, J. Hait and B. D. Pandey, *Waste management*, 2013, **33**, 1890.
11. S. Zhu, W. He, G. Li, X. Zhou, X. Zhang and J. Huang, *Transactions of Nonferrous Metals Society of China*, 2012, **22**, 2274.
12. B. Xin, D. Zhang, X. Zhang, Y. Xia, F. Wu, S. Chen and L. Li, *Bioresource Technology*, 2009, **100**, 6163.
13. D. Mishra, D. Kim, D. E. Ralph, J. Ahn and Y. Rhee, *Waste Management*, 2008, **28**, 333.
14. G. Zeng, X. Deng, S. Luo, X. Luo and J. Zou, *Journal of hazardous materials*, 2012, **199-200**, 164.
15. L. Ma, Z. Nie, X. Xi and X. Han, *Hydrometallurgy*, 2013, **136**, 1.
16. L. Li, R. Chen, F. Sun, F. Wu and J. Liu, *Hydrometallurgy*, 2011, **108**, 220.
17. L. Yang, Q. Yan, G. Xi, L. Niu, T. Lou, T. Wang, X. Wang, *J Mater Sci*, 2011, **46**, 6106.
18. M. Joulié, R. Laucournet and E. Billy, *Journal of Power Sources*, 2014, **247**, 551.
19. L. Li, J. B. Dunn, X. Zhang, L. Gaines, R. Chen, F. Wu and K. Amine, *Journal of Power Sources*, 2013, **233**, 180.
20. Y. Deng, L. Wan, Y. Xie, X. Qin and G. Chen, *RSC Adv.*, 2014, **4**, 23914.
21. Q. Zhang, T. Peng, D. Zhan, X. Hu and G. Zhu, *Materials Chemistry and Physics*, 2013, **138**, 146.
22. M. Wang, G. Lei, J. Hu, K. Liu, S. Sang and H. Liu, *RSC Adv.*, 2014, **4**, 62615.
23. L. Li, Z. Chen, Q. Zhang, M. Xu, X. Zhou, H. Zhu and K. Zhang, *J. Mater. Chem. A*, 2015, **3**, 894.
24. R. Tian, G. Liu, H. Liu, L. Zhang, X. Gu, Y. Guo, H. Wang, L. Sun and W. Chu, *RSC Adv.*, 2015, **5**, 1859.
25. M. B. Sahana, S. Vasu, N. Sasikala, S. Anandan, H. Sepehri-Amin, C. Sudakar and R. Gopalan, *RSC Adv.*, 2014, **4**, 64429.
26. J. Li, S. Xiong, Y. Liu, Z. Ju and Y. Qian, *Nano Energy*, 2013, **2**, 1249.
27. S. Akimoto and I. Taniguchi, *Journal of Power Sources*, 2013, **242**, 627.
28. A. Mahmoud, I. Saadoune, J.M. Amarilla, R. Hakkou, *Electrochimica Acta*, 2011, **56**, 4081.
29. E. Shinova, R. Stoyanova, E. Zhecheva, G. Ortiz, P. Lavela and J. Tirado, *Solid State Ionics*, 2008, **179**, 2198.
30. M. Sivakumar, A. Towata, K. Yasui, T. Tuziuti, T. Kozuka, Y. Iida, M. M. Maiorov, E. Blums, D. Bhattacharya, N. Sivakumar and M. Ashok, *Ultrasonics Sonochemistry*, 2012, **19**, 652.
31. G. Chen, X. Tang, Z. Wang, Q. Yi, L. Chen, Y. Xiao, *Chinese Journal of Inorganic Chemistry*, 2011, **27**, 1987.
32. C. Hu, J. Guo, J. Wen and Y. Peng, *J. Mater. Sci. Technol.*, 2013, **29**, 215.
33. K.M. Shaju, G. V. Subba Rao. B.V.R. Chowdari, *Electrochimica Acta*, 2002, **48**, 145.
34. L. Chen, X. Tang, Y. Zhang, L. Li, Z. Zeng and Y. Zhang, *Hydrometallurgy*, 2011, **108**, 80.
35. D. A. Ferreira, L. M. Z. Prados, D. Majuste and M. B. Mansur, *Journal of Power Sources*, 2009, **187**, 238.
36. H. Zou, E. Gratz, D. Apelian and Y. Wang, *Green Chemistry*, 2013, **15**, 1183.
37. G. P. Nayaka, J. Manjanna, K. V. Pai, R. Vadavi, S.J.Keny and V.S.Tripathi, *Hydrometallurgy*, 2015, **151**, 73.
38. K. M. Nam, H. J. Kim, D. H. Kang, Y. S. Kim and S. W. Son, *Green Chemistry*, 2015, **17**, 1127.
39. B. J. Hwang, Y. W. Tsai, D. Carlier and G. Ceder, *Chem. Mater.*, 2003, **15**, 3676.
40. J. Song, L. Wang, Z. Ma, Z. Du, G. Shao, L. Kong, and W. Gao, *RSC Adv.*, 2015, **5**, 1983.
41. Y. Ding, J. Xie, G. Cao, T. Zhu, H. Yu and X. Zhao, *Adv. Funct. Mater.*, 2011, **21**, 348.
42. X. Yi, X. Wang, B. Ju, Q. Wei, X. Yang, G. Zou, H. Shu and L. Hu, *Journal of Alloys and Compounds*, 2014, **604**, 50.

Re-synthesis of new cathode material from waste LIBS using citric acid as leaching agent and complexing agent

